SCIENCE CHINA
Physics, Mechanics & Astronomy

• Article •

September 2025 Vol. 68 No. 9: 298211
https://doi.org/10.1007/s11433-025-2690-9

Atomic cubic gauche nitrogen polymerized at ambient pressure

Runteng Chen[1†], Jun Zhang[1,2*†], Zelong Wang[1], Ke Lu[1], Yi Peng[1], Jianfa Zhao[1,2], Shaomin Feng[1,2], and Changqing Jin[1,2*]

[1] *Beijing National Laboratory for Condensed Matter Physics, Institute of Physics, Chinese Academy of Sciences, Beijing 100190, China*
[2] *School of Physics, University of Chinese Academy of Sciences, Beijing 100190, China*

Received January 18, 2025; accepted May 14, 2025; published online June 20, 2025

Polymeric nitrogen has long been pursued as a high-energy density material but is very challenging to synthesize at ambient pressure conditions especially with light element precursors. Using a developed one pot method, we successfully synthesized the atomic polymeric nitrogen employing lithium azide as a precursor. Raman spectrum measurements detected the emerging vibrational peak at 635 cm^{-1} for the polymerized lithium azide sample, indicating the formation of atomic cubic gauche nitrogen (cg-N) with N–N single bonds. Through systematic investigations, the preparation conditions are optimized to be 180°C with a reaction time of 3 h for obtaining atomic cubic gauche polymeric nitrogen. The one pot method achieves the quantitative synthesis of cg-N at ambient pressure using alkali metal azide as the precursors. It offers a simple way for further scalable synthesis of polymeric atomic nitrogen high energy density materials.

cubic gauche polymeric nitrogen (cg-N), lithium azide, thermal stability

PACS number(s): 74.62.Bf, 36.20.Ng, 61.50.Ks, 81.16.Be

Citation: R. Chen, J. Zhang, Z. Wang, K. Lu, Y. Peng, J. Zhao, S. Feng, and C. Jin, Atomic cubic gauche nitrogen polymerized at ambient pressure, Sci. China-Phys. Mech. Astron. **68**, 298211 (2025), https://doi.org/10.1007/s11433-025-2690-9

1 Introduction

The polymeric nitrogen consisting of N–N single bonds and N=N double bonds is considered a high energy density material due to the significant energy difference upon decomposition into stable nitrogen gas with N≡N triple bonds [1]. For the atomic polymeric nitrogen materials with complete N–N single bonds, the chemical energy of about 800 kJ/mol is expected to be released during decomposition into nitrogen molecules [2]. Therefore, single bonded polymeric nitrogen as a promising high energy density material attracts lots of attention in the research of explosives or propellants.

In the past few decades, tremendous progress has been made in the research of polymeric nitrogen. McMahan et al. [3] initially proposed preparation of the monatomic polymeric nitrogen by compressing the molecular nitrogen in 1985 and then Mailhiot et al. [4] predicted the cubic gauche nitrogen (cg-N) using the global potential energy surface search method. Later continuous endeavors were made to seek the N–N single-bonded polymeric nitrogen [5,6]. The experimental breakthrough came in 2004 when Eremets et al. [1,7] prepared cg-N by directly compressing molecular nitrogen gas at pressures above 110 GPa with heating temperatures above 2000 K. Inspired by this work, a large amount of theoretical work predicted the existence of polymeric nitrogen with new structures consisting of N–N single bonds at high pressure [8-23]. Experimentally the layered structure [24], the hexagonal layered structure [25], the black phosphorus-like nitrogen [26], and the Panda nitrogen [27]

†Equally contributed to this work
*Corresponding authors (Jun Zhang, email: zhang@iphy.ac.cn; Changqing Jin, email: jin@iphy.ac.cn)

were successfully prepared at the pressure above 120 GPa. However, all these polymeric nitrogen materials are synthesized at high pressure and cannot be recovered to ambient pressure that challenges the physical properties and application research.

Theoretical study indicates that the cg-N structure might exist as a metastable phase at ambient pressure [14,28]. In recent years, the polymeric nitrogen materials have been successfully prepared at ambient pressure using sodium azide as a precursor [29-34] by the plasma enhanced chemical vapor deposition (PECVD) technique. In principle, the formation of cg-N is accompanied by the coprecipitation of alkali metal or by-products with metal azide precursors, which may hinder the chemical reaction. The separation of heavier alkali metal, such as sodium and potassium or related byproducts with cg-N produced is challenged, further restricting the application of cg-N due to the less cg-N in the product. Therefore, a new technique is strongly desirable to synthesize the cg-N with a lighter precursor at a mild condition.

Very recently a one pot synthesis method was developed to prepare cg-N with a high yield by heating the alkali metal azide precursors [35,36]. Although it is considered that azide ions play a critical role in the formation of cg-N, the properties of alkali metal ions, particularly their different radii, can influence the stability of chemical bond within azide ions [37]. In our recent experiments, the optimized synthesis temperatures for cg-N are 240°C-260°C and 290°C-300°C, respectively, when sodium and potassium azide were employed as precursors [35,36]. This should result from the stronger polarization effect on azide ions exerted by the alkali metal ions as their radii decrease. By contrast, the more serious polarizability or shift of electron cloud of azide ion can drastically change the bonding trend of alkali metal elements and the thermal stability of alkali metal azides. Thus, alkali metal ion with smaller radii can destabilize the N=N bonds in azide ions, favoring the formation of cg-N at mild conditions. As proposed by theory, the transition path to polymeric nitrogen may pass through different molecular structures that have limited thermodynamic stability [38]. Further, the byproducts with a small weight that form simultaneously with cg-N are expected. Lithium is the lightest metal, and thus, when lithium azide is employed to synthesize cg-N, it is expected that cg-N will have the highest mass content in the synthesized products, favoring its applications as a high energy density material. Therefore, lithium azide is an ideal candidate for preparing cg-N. We hereby report the synthesis of cg-N using one pot method employing lithium azide as a precursor.

2 Materials and methods

Lithium azide (LiN_3) solution (Sigma Aldrich, 20 wt% in water) was used as the nitrogen source to synthesize cg-N. The solution of LiN_3 was first dropped into a crucible. Then the crucible was transferred into a tubular furnace. The optimized synthesis conditions with a reaction temperature of 180°C and a heating time of 3 h under vacuum conditions were employed to synthesize the cg-N. The sample was named as "polymerized lithium azide (PLA)" followed by synthesis temperature and duration, like PLA-180°C-3 h.

The Raman spectra were recorded in the range of 100-1500 cm^{-1} with a spectral resolution of 1 cm^{-1} using integrated laser Raman system (Renishaw) with a confocal microscope and multichannel air-cooled CCD detector. The semiconductor lasers with 532 nm excitation wavelength and Olympus SLMPLN 20×0.25 objective were used. In general, the measurement conditions, including diffraction grating of l/2400 mm (vis), exposure time of 30 s, laser power of 1%, accumulations of 3 times were preferred. Thermogravimetric (TG) analysis and differential scanning calorimetry (DSC) techniques are employed to characterize the thermal stability. The data were collected using a Simultaneous Thermal Analyzer (HENVEN HCT-4) in Argon gas atmosphere with a purity of 5N according to a heating rate of 10°C/min.

3 Results

Figure 1 shows the crystal structure of cg-N, where each nitrogen atom bonds to three nearest counterparts through N–N single bonds with equal distances, and the leftover *p* orbital is occupied by lone pair electrons (depicted on the right in Figure 1). The single-bonded nitrogen atoms connect to each other to form a three-dimensional network structure [39], as shown in the left panel of Figure 1. Thus, cg-N adopts a body-centered-cubic Bravais lattice and belongs to $I\,2_13$ space group. The lattice constant of cg-N was extrapolated to be 3.77 Å [7] at ambient pressure conditions and the N–N bond length is predicted to be 1.40 Å [4,40,41]. According to the lattice constant, the diffraction peak of (011) with the highest intensity should center at ~33.56° when Cu Kα irradiation is employed, which will be discussed further later.

As reported by Eremets et al. [1] a high pressure exceeding 110 GPa was required for the synthesis of cg-N through the compression of triply bonded dinitrogen. This should be

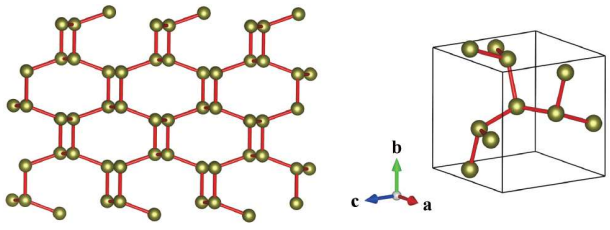

Figure 1 (Color online) Crystal structure for the single bonded cg-N.

ascribed to the large energy barrier between triply bonded dinitrogen and single bonded N–N. Therefore the azide ion composed of N=N double bonds with a dissociation energy of 417 kJ/mol (less than one half of that in N≡N) is an ideal precursor for synthesizing the cg-N due to the low energy barrier involved in transforming N=N double bonds into singly bonded cg-N [2,3]. For the alkali metal azides, lithium ions with the smallest radius are expected to show the strongest polarization effect to azide ion, which leads to a lower energy requirement for dissociating the N=N double bonds in azide ions. Therefore, lithium azide is a better candidate to synthesize polymeric nitrogen. The Raman spectrum is sensitive to the subtle changes of crystal structure and composition and is used to detect the formation of polymeric nitrogen by examining the characteristic peaks corresponding to the N–N single bond.

The synthesis temperatures of cg-N were first investigated. The Raman spectra of PLA synthesized at 150°C-210°C with a reaction time of 3 h are shown in Figure S1 (Supporting Information). As for the PLA-150°C sample, the sharp peaks of LiN_3 are observed near 118 cm^{-1}, 1357 cm^{-1}, and 1371 cm^{-1} similar to those in sodium and potassium azides [31,34,42]. These peaks can be assigned to the vibrational lattice mode, the first overtone of the IR-active bending ν2 mode, and the symmetric stretching ν1 mode of the azide ion, respectively. As the reaction temperature increases, the PLA samples synthesized from 160°C to 200°C exhibit emerging vibrational peaks at 635 cm^{-1}, which was accompanied by the dramatic changes in peak profiles at 1357 cm^{-1} and 1371 cm^{-1}. For example, the peaks at 1357 cm^{-1} and 1371 cm^{-1} merged in the PLA-160°C sample, which was exhibited by an asymmetric peak centered at 1350 cm^{-1}. Figure 2 shows the typical Raman spectrum for the PLA-180°C-3 h sample. The vibrational peak at 635 cm^{-1} for PLA-180°C-3 h sample is comparable to the reported results for the synthesized cg-N samples when sodium azide and potassium azide were used as precursors in our previous experiments [35,36]. When extrapolating the high pressure data to ambient pressure [1,40,41], the near linear pressure dependence of vibrational positions overlaps well with our present data indicated by the blue pentagram in the inset of Figure 2.

According to group theory analysis, the 12 optical modes in the zone center of the cubic gauche structure are decomposed into A+E+2T modes. The T modes are both Raman and infrared active, and the A and E modes are only Raman active. Therefore, four vibrational modes of the cg-N crystal are present [28,40,41]. Further, theoretical work calculated the relative intensity of Raman peaks of cg-N and proposed that the Raman spectra are dominated by the A mode. The intensity of the other modes is less than 10% and consequently they would be hardly observable in a measurement [41]. Our experimental measurements are in excellent

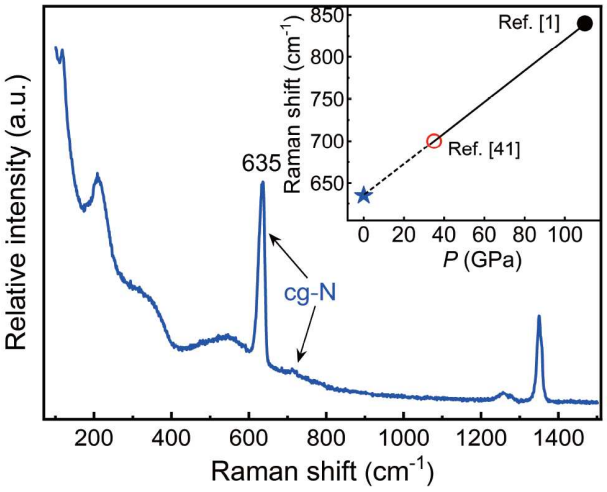

Figure 2 (Color online) Raman spectra for the polymerized atomic nitrogen sample based on lithium azide (PLA) synthesized at 180°C with a heating time of 3 h. The Raman spectra show new peaks at 635 cm^{-1} and 700 cm^{-1}, which characterize the formation of cg-N. Inset shows the pressure dependence of Raman fingerprint peak position for cg-N, including the experimental data at 110 GPa (solid circle) and the calculated vibrational position at 35 GPa (open circle) of cg-N dominated by the A mode extracted from refs. [1,41], respectively. The Raman vibrational position of cg-N can be extrapolated to ambient pressure as shown by the dashed line, which overlaps well with our present data indicated by the blue pentagram.

agreement with the theoretical findings, in terms of both peak position and intensity. In our experiments, we observe a main Raman peak located at 635 cm^{-1} and a very weak peak at 700 cm^{-1}, which can be definitively assigned to the pore breathing A symmetry and N–N tilting T (TO) symmetry Raman-active modes, respectively, of cg-PN extrapolated to ambient pressure according to the calculation [41]. In addition, the asymmetric broadening of Raman peak profiles at 635 cm^{-1} for the PLA samples is observed, which should correspond to the variant of secondary-structure. For example, the cg-N forms nanocrystals [43] and will be discussed later.

Figure 3(a) and Figure S1 show that the vibrational intensities of cg-N increase as the reaction temperature rises from 160°C to 180°C, compared to those at 1350 cm^{-1} for the unreacted LiN_3 in the PLA samples. As the temperature increases to 190°C, the Raman intensity of cg-N remains comparable (shown in Table S1, Supporting Information) and then decreases significantly at 200°C. Significant volatilization of LiN_3 was observed when the synthesis temperature increased to 210°C, and only a little sample was left in the experiment, albeit the occasional presence of cg-N. Often the peak profile becomes indistinguishable at 210°C, as shown in Figure S1. That is, the growth of cg-N is restricted by the boiling point of lithium azide in the present synthesis route, where the vacuum condition is applied. Therefore the optimized temperature for synthesizing cg-N is

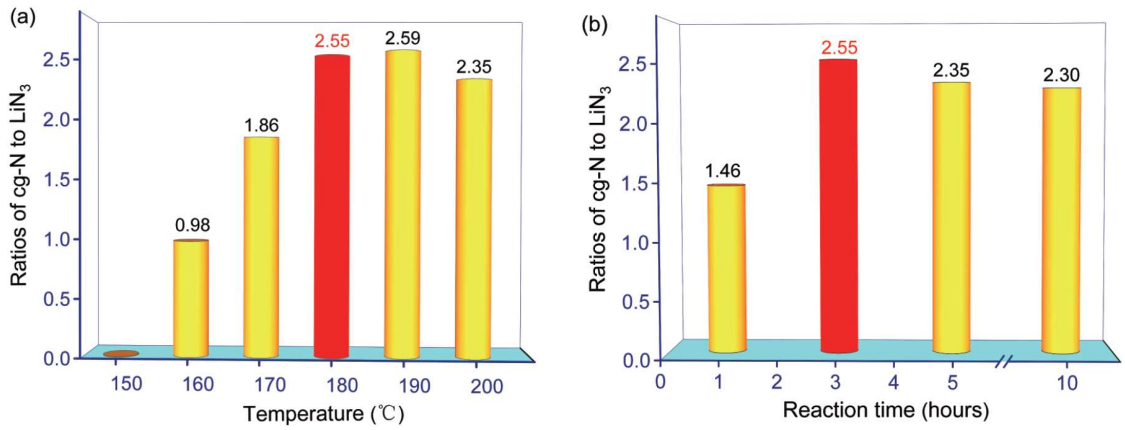

Figure 3 (Color online) (a) Synthesis temperature as a function of the conversion ratios for the PLA samples synthesized between 150°C-200°C with a heating time of 3 h; (b) the reaction time as a function of the conversion ratios for the PLA samples synthesized at 180°C with a reaction time up to 10 h. The optimized synthesized conditions of 180°C with a reaction time of 3 h for PLA sample are indicated by the red cylinder.

approximately 180°C when using LiN_3 as a precursor. After the reaction, PLA samples exhibit a uniformly dark red or black color that should be related to the by-product Li_3N, which forms concurrently with the cg-N growth. Here the abundance of the cg-N phase in PLA samples synthesized at different temperatures was quantitatively calculated. A simplified conversion degree or conversion ratio from LiN_3 to cg-N is defined based on the characteristic peak intensity ratios. Table S1 summarizes partial vibrational intensities of LiN_3 and cg-N. The peak intensity at 635 cm^{-1} is used to reflect the amount of cg-N synthesized while the peak intensity at 1350 cm^{-1} represents the amount of unreacted LiN_3. The intensity ratios were calculated using the formula $(I_{635}–I_{bg})/(I_{1350}–I_{bg})$, in which the background is extracted from the linear part near 1400 cm^{-1}. The properties of unreacted LiN_3 in PLA samples were firstly evaluated using the formula $(I_{118}–I_{bg})/(I_{1350}–I_{bg})$. The ratios are approximately 3 for the PLA samples synthesized at 170°C-200°C, indicating the similar state for LiN_3. The peak intensity ratios of cg-N to LiN_3 increase to 2.55-2.59 as synthesis temperature increases to 180°C-190°C and then decreases at higher temperatures. The temperature dependence of the conversion ratios of cg-N is shown in Figure 3(a), where an inverted U curve further indicates the optimized synthesis temperature of 180°C-190°C for the PLA samples. It is noteworthy that the PLA samples synthesized at 190°C show large intensity discrepancy in the Raman measurement as detection sites change, indicating the inhomogeneity in the PLA samples.

Further, the preparation conditions for cg-N were explored to synthesize PLA samples at 180°C with variable reaction times. The Raman vibrational intensities of cg-N in the PLA-180°C samples increase gradually as the reaction time extends up to 3 h and then decreases, as shown in Figure S2. The detailed peak intensities and ratios of cg-N to LiN_3 are summarized in Table S2. The sample prepared at 180°C with a reaction time of 3 h shows higher conversion to cg-N, and extending the reaction time does not improve the conversion as shown in Figure 3(b). The integral areas of characteristic peaks for cg-N at 635 cm^{-1} and LiN_3 at 1350 cm^{-1} were further calculated to confirm the conversion ratios. The data are included in Table S3. It is clear that the ratios calculated by peak areas and intensities show consistent results. Therefore the optimized preparation conditions for cg-N are 180°C with a reaction time of 3 h when using lithium azide as a precursor.

The thermal stability is a crucial property for the application of high energetic density materials. The TG-DSC measurements were performed for the PLA-180°C-3 h sample. As shown in Figure 4, after several experiments, the exothermic peaks centered at 302°C and 576°C can be well reproduced, which undoubtedly derive from the decomposition of LiN_3 unreacted and the by-product Li_3N in the PLA-180°C-3 h sample, respectively. The emergence of a new peak centered at 428°C should be related to the cg-N synthesized. The mass losses were also observed at all those exothermic temperatures, further confirming the decomposition of LiN_3, cg-N, and Li_3N, respectively. The TG curve was enlarged and shown in the inset of bottom panel. After carefully examining, ~1 wt% loss at 428°C was confirmed, corresponding to the content of cg-N in the PLA-180°C-3 h sample. It is still a higher yield reported to date when cg-N is synthesized at ambient conditions. It is worth noting that the decomposition temperature of cg-N highly depends on the sample state and measurement conditions, ranging from 420°C-490°C. As proposed above in analyzing the Raman peak profiles, the cg-N may exist in the form of nanocrystals with variable sizes and activation energy, which directly determine the decomposition temperature of cg-N prepared. As reported in the published work, the cg-N decomposes at 488°C, 477°C, and 448°C, respectively, albeit similar

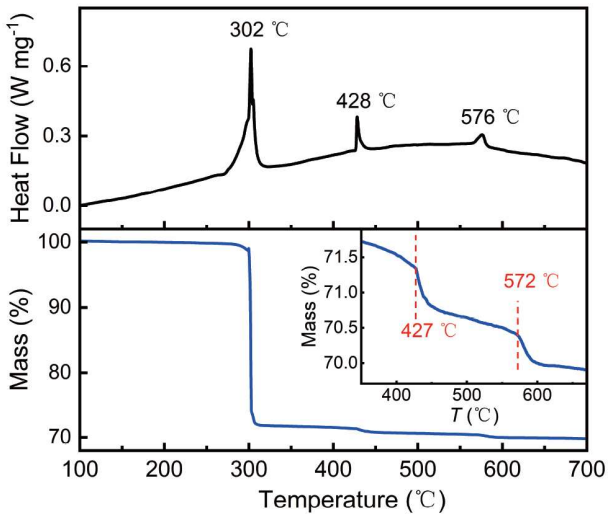

Figure 4 (Color online) TG-DSC curves for the polymerized atomic nitrogen sample based on lithium azide synthesized at 180°C with a reaction time of 3 h (PLA-180°C-3 h). The temperature dependence of TG and DSC curves are shown in blue and black lines, respectively. The exothermic peaks at 302°C, 428°C, and 576°C correspond to the decomposition of LiN_3 unreacted, cg-N produced, and Li_3N by-product in PLA sample. Inset in the bottom panel shows the enlarged view to give mass loss threshold at approximately 427°C for the cg-N synthesized.

synthesis routes were employed [34,35,42]. Besides, the types and content of unreacted precursors and by-products in the mixture used in TG-DSC measurement also have an important influence on the thermal stability of cg-N samples. Therefore, the exothermic peak at 428°C is from the decomposition of cg-N prepared by one pot method using LiN_3 as a precursor.

4 Discussion

The cg-N can be synthesized via a one pot synthesis method using alkali metal azides, including lithium (the present work), sodium, and potassium azides as precursors that correspond to the optimized synthesis temperatures of 180°C-190°C, 240°C-260°C [36], and 290°C-300°C [35], respectively. That is, the formation of cg-N is based on the azide ions. The lowered temperature for cg-N synthesis using lithium azide precursor further confirms the decreased dissociation energy for the azide ions, which derives from the more serious polarization effect of the alkali metal ion on azide ions as they evolve from K^+ to Li^+. However, the polarization effect directly influences the lattice energy, and thereby the boiling point of alkali metal azides. The large polarizability on the azide ions exerted by lithium ions leads to serious volatility, detrimental to the successful preparation of cg-N. Therefore, the high pressure technique that can suppress the volatility of alkali metal azides would be well compatible with the high yield of cg-N.

The full width at half maxima (FWHM) of the Raman peaks at 635 cm^{-1} for characterizing cg-N for the PLA samples are listed in Table S3. It is found that the values of FWHM are approximately 19 cm^{-1} for the PLA samples synthesized at 160°C-190°C with a reaction time of 3 h and for those synthesized at 180°C with a reaction time of 3-5 h. These results are consistent with the optimized synthesis conditions. On the contrary, those prepared at a temperature above 190°C, or less or more than 3 h led to a decrease in FWHM accompanied by a decreased phase content of cg-N. The above experimental observations conclude that cg-N exists in a nanocrystalline form in the PLA samples. The higher temperatures favor the growth of cg-N nanoparticles as reported in our work [31] where the cg-N exhibits a higher conversion ratio at 300°C when using potassium azide as a precursor. The peak profiles of cg-N prepared are further carefully examined. It is also found that the peaks at 635 cm^{-1} were unsymmetrically distributed; this indicates the presence of cg-N crystalline with variable sizes, which may be closely related to the growth mechanism of cg-N. That is, cg-N initially crystallizes based on the azide ions to form the nanocrystalline and then grows with broad particle sizes distribution.

Upon polymerized reaction, the samples exhibit a dark red color for the PLA samples that correspond to the by-products Li_3N as indicated by our preliminary DSC measurements. The cg-N obtained is stable at least up to 427°C at ambient pressure. The proposed transformation route from alkali metal (M) azides to cg-N may be as: (1) $MN_3 \rightarrow$ cg-N + M_3N; (2) $M_3N \rightarrow M + N_2$ while the differences between the potassium azide and lithium or sodium counterparts are determined by the stability of by product M_3N. In our X-ray diffraction experiment, no diffraction peaks were found at 33.56°, which corresponds to the theoretically most intense reflection under ambient pressure conditions. The possible explanations are the inherently small scattering cross-section of nitrogen atoms for X-rays, the low cg-N content (~1 wt% as determined by TG mass loss measurements), and peak broadening caused by the nanocrystalline nature of cg-N, which together result in an undetectable diffraction signal. Different from the sodium and potassium azides, the by-products Li_3N or metal Li with lighter molecular weight are expected to impose less influence to the applications of cg-N synthesized. It is well known that lithium has a low melting point and excellent ignition performance [44]. The combustion heat of lithium is 42.94 kJ/g, much higher than potassium of 4.65 kJ/g [45]. The present synthesis of cg-N has been achieved experimentally under ambient pressure, which shows significant promise for scaling up its production. Based on theoretical predictions, cg-N could provide record-breaking specific impulse values of 510-513 s [45] and a tenfold improvement in detonation pressure compared to HMX [46]. Therefore, polymeric nitrogen, as a novel high

energy density material, shows great potential for application in the fields of explosives and propellants.

Although the preparation method presented in this work has achieved the synthesis of polymeric nitrogen at ambient pressure, the phase content is insufficient to support the need for structural characterization. In addition, the synthesis of cg-N is accompanied by the formation of byproducts, which results in a mixture containing cg-N. Therefore, synthesizing pure polymeric nitrogen or improving purity at ambient pressure remains a challenge.

5 Conclusion

In this work, a one pot synthesis method was successfully applied to prepare polymerized atomic cg-N using lithium azide as a precursor. The cg-N sample was obtained at 180°C with a reaction time of 3 h, characterized by Raman spectra. It remains stable at least up to 427°C. The technique is promising for further scaling up of polymeric nitrogen materials, including cg-N at ambient pressure. Further investigation into the physical mechanisms with respect to stability at ambient pressure is desirable for improving the quality of polymeric nitrogen, which will facilitate the transition of polymeric nitrogen materials from basic research to applied research.

This work was supported by the National Key R&D Program of China (Grant No. 2023YFA1406000), and the CAS Project for Young Scientists in Basic Research (Grant No. YSBR-052).

Conflict of interest The authors declare that they have no conflict of interest.

Supporting Information

The supporting information is available online at http://phys.scichina.com and https://link.springer.com. The supporting materials are published as submitted, without typesetting or editing. The responsibility for scientific accuracy and content remains entirely with the authors.

1 M. I. Eremets, A. G. Gavriliuk, I. A. Trojan, D. A. Dzivenko, and R. Boehler, Nat. Mater **3**, 558 (2004).
2 P. C. Samartzis, and A. M. Wodtke, Int. Rev. Phys. Chem. **25**, 527 (2006).
3 A. K. McMahan, and R. LeSar, Phys. Rev. Lett. **54**, 1929 (1985).
4 C. Mailhiot, L. H. Yang, and A. K. McMahan, Phys. Rev. B **46**, 14419 (1992).
5 E. Gregoryanz, A. F. Goncharov, R. J. Hemley, and H. Mao, Phys. Rev. B **64**, 052103 (2001).
6 A. F. Goncharov, E. Gregoryanz, H. Mao, Z. Liu, and R. J. Hemley, Phys. Rev. Lett. **85**, 1262 (2000).
7 M. I. Eremets, A. G. Gavriliuk, and I. A. Trojan, Appl. Phys. Lett. **90**, 171904 (2007).
8 M. M. G. Alemany, and J. L. Martins, Phys. Rev. B **68**, 024110 (2003).
9 W. D. Mattson, D. Sanchez-Portal, S. Chiesa, and R. M. Martin, Phys. Rev. Lett. **93**, 125501 (2004).
10 K. Nordlund, A. Krasheninnikov, N. Juslin, J. Nord, and K. Albe, Europhys. Lett. **65**, 400 (2004).
11 F. Zahariev, A. Hu, J. Hooper, F. Zhang, and T. Woo, Phys. Rev. B **72**, 214108 (2005).
12 F. Zahariev, S. V. Dudiy, J. Hooper, F. Zhang, and T. K. Woo, Phys. Rev. Lett. **97**, 155503 (2006).
13 A. R. Oganov, and C. W. Glass, J. Chem. Phys. **124**, 244704 (2006).
14 T. Zhang, S. Zhang, Q. Chen, and L. M. Peng, Phys. Rev. B **73**, 094105 (2006).
15 F. Zahariev, J. Hooper, S. Alavi, F. Zhang, and T. K. Woo, Phys. Rev. B **75**, 140101 (2007).
16 H. Katzke, and P. Tolédano, Phys. Rev. B **78**, 064103 (2008).
17 Y. Yao, J. S. Tse, and K. Tanaka, Phys. Rev. B **77**, 052103 (2008).
18 Y. Ma, A. R. Oganov, Z. Li, Y. Xie, and J. Kotakoski, Phys. Rev. Lett. **102**, 065501 (2009).
19 C. J. Pickard, and R. J. Needs, Phys. Rev. Lett. **102**, 125702 (2009).
20 B. Boates, and S. A. Bonev, Phys. Rev. Lett. **102**, 015701 (2009).
21 B. Boates, and S. A. Bonev, Phys. Rev. B **83**, 174114 (2011).
22 X. Wang, Y. Wang, M. Miao, X. Zhong, J. Lv, T. Cui, J. Li, L. Chen, C. J. Pickard, and Y. Ma, Phys. Rev. Lett. **109**, 175502 (2012).
23 A. A. Adeleke, M. J. Greschner, A. Majumdar, B. Wan, H. Liu, Z. Li, H. Gou, and Y. Yao, Phys. Rev. B **96**, 224104 (2017).
24 D. Tomasino, M. Kim, J. Smith, and C. S. Yoo, Phys. Rev. Lett. **113**, 205502 (2014).
25 D. Laniel, G. Geneste, G. Weck, M. Mezouar, and P. Loubeyre, Phys. Rev. Lett. **122**, 066001 (2019).
26 C. Ji, A. A. Adeleke, L. Yang, B. Wan, H. Gou, Y. Yao, B. Li, Y. Meng, J. S. Smith, V. B. Prakapenka, et al., Sci. Adv. **6**, eaba9206 (2020).
27 L. Lei, Q. Q. Tang, F. Zhang, S. Liu, B. B. Wu, and C. Y. Zhou, Chin. Phys. Lett. **37**, 068101 (2020).
28 T. W. Barbee, Phys. Rev. B **48**, 9327 (1993).
29 H. Abou-Rachid, A. Hu, V. Timoshevskii, Y. Song, and L. S. Lussier, Phys. Rev. Lett. **100**, 196401 (2008).
30 E. M. Benchafia, C. Yu, M. Sosnowski, N. M. Ravindra, and Z. Iqbal, JOM **66**, 608 (2014).
31 E. M. Benchafia, Z. Yao, G. Yuan, T. Chou, H. Piao, X. Wang, and Z. Iqbal, Nat. Commun. **8**, 930 (2017).
32 H. Zhuang, S. Alzaim, S. Li, E. M. Benchafia, J. Young, N. M. Ravindra, Z. Iqbal, and X. Wang, Chem. Mater. **34**, 4712 (2022).
33 C. Qu, J. Li, K. Ding, S. Guo, and Y. Jia, Molecules **29**, 504 (2024).
34 Y. Xu, G. Chen, F. Du, M. Li, L. Wu, D. Yao, X. Liu, J. Ding, Z. Zeng, R. Liu, et al., Sci. Adv. **10**, eadq5299 (2024).
35 R. Chen, J. Zhang, Z. Wang, K. Lu, Y. Peng, J. Zhao, X. Liu, S. Feng, R. Liu, C. Xiao, et al., Sci. Bull. **69**, 3812 (2024).
36 R. Chen, J. Zhang, Z. Wang, K. Lu, Y. Peng, J. Zhao, S. Feng, and C. Jin, Chin. Phys. Lett. **41**, 126102 (2024).
37 X. Wang, J. Li, J. Botana, M. Zhang, H. Zhu, L. Chen, H. Liu, T. Cui, and M. Miao, J. Chem. Phys. **139**, 164710 (2013).
38 R. Caracas, and R. J. Hemley, Chem. Phys. Lett. **442**, 65 (2007).
39 D. Plašienka, and R. Martoňák, J. Chem. Phys. **142**, 094505 (2015).
40 J. Zhao, Phys. Lett. A **360**, 645 (2007).
41 R. Caracas, J. Chem. Phys. **127**, 144510 (2007).
42 L. Wu, Y. Xu, G. Chen, J. Ding, M. Li, Z. Zeng, and X. Wang, Chin. Phys. B **33**, 126802 (2024).
43 Y. Gao, and P. Yin, Sci. Rep. **7**, 43602 (2017).
44 W. Xiong, Y. Liu, T. Zhang, S. Wu, D. Zeng, X. Guo, and A. Pang, Aerospace **10**, 222 (2023).
45 V. E. Zarko, Combust. Explos. Shock Waves **46**, 121 (2010).
46 K. O. Christe, Propellants Explos. Pyrotec. **32**, 194 (2007).